IEEE Photonics Journal
An IEEE Photonics Society Publication

Open Access

Improved 808-nm High-Power Laser Performance With Single-Mode Operation (Vertical Direction) in Large Optical Cavity Waveguide

Volume 10, Number 2, April 2018

Bocang Qiu
H. Martin Hu
Weimin Wang
Wenbin Liu
Shujuan Wu
Zhiguo Song
Xue Bai

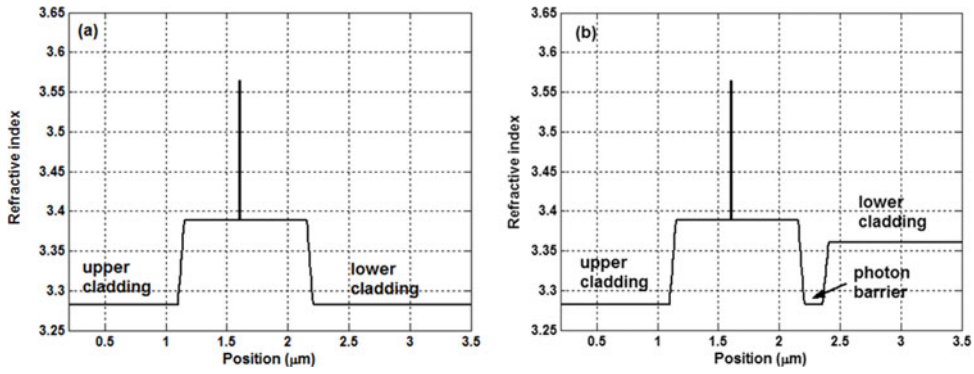

DOI: 10.1109/JPHOT.2018.2810125
1943-0655

IEEE photonics SOCIETY

IEEE

Improved 808-nm High-Power Laser Performance With Single-Mode Operation (Vertical Direction) in Large Optical Cavity Waveguide

Bocang Qiu,[1,3] **H. Martin Hu**,[1,3] **Weimin Wang**,[2] **Wenbin Liu**,[2] **Shujuan Wu**,[2] **Zhiguo Song**,[2] **and Xue Bai** [2]

[1]The Research Institute of Tsinghua University in Shenzhen, Shenzhen 518055, China
[2]Raybow Optoelectronics Ltd. Inc., Shenzhen 518055, China
[3]Guangdong Provincial Key Laboratory of Optomechatronics, Shenzhen 518057, China

DOI:10.1109/JPHOT.2018.2810125

Manuscript received January 3, 2018; revised February 1, 2018; accepted February 22, 2018. Date of publication February 27, 2018; date of current version March 23, 2018. This work was supported in part by the National High Technology Research and Development Program (863 Program) "High Linearity and High Saturation Power Laser Photodetector Array Chip" under Grant 2015AA016901, in part by the Committee for Science and Technology Innovation of Shenzhen via the research project of "Development of High Performance High-Power Twin Junction InGaAlAs 1550 nm Lasers (JSGG20160301095954267)," in part by the Innovative R&D Team Leadership Guangdong Province Program, and in part by the Shenzhen City Peacock Program. Corresponding author: Xue Bai (e-mail: baixue@raybowlaser.com).

Abstract: We present a detailed study of the effect of large optical cavity (LOC) waveguide design on the laser's kink performance and it was found that a multimode waveguide in the epi growth direction could lead to the occurrence of the power kink in the light–current (*L–I*) curve, and the occurrence of the power kink was accompanied with the broadening of the beam divergence in the wafer growth direction. In order to eliminate the kink issue that is associated with the lasing of the higher-order modes, a new type of waveguide, which is called higher-order-mode tunneling waveguide, was proposed in our design. The new type of waveguide can strongly promote the leakage of higher-order modes, and in this way, the LOC waveguide becomes single-moded. Test of the fabricated devices based on the new design showed that the devices indeed exhibited perfect *L–I* linearity without kinks.

Index Terms: High power semiconductor lasers, large optical cavity, single mode waveguide.

1. Introduction

High power semiconductor lasers emitting at the wavelength of 808 nm have a number of important applications, including solid state laser pumping and material processing. The concept of Large optical cavity (LOC) waveguide was first proposed by Lockwood et al in 1970 [1], and since then has been widely used in a variety of high power semiconductor laser structures [2]–[6], because it offers very low optical loss, leading to improved energy conversion efficiency (ECE), which is one of the most important considerations in designing high power lasers. For many applications in which fiber coupling and other coupling optics are used, it is required that semiconductor lasers are able to produce a stable beam property and good light-current L-I linearity. In contrast to a narrow waveguide design, the waveguide thickness in LOC designs is much thicker and can be

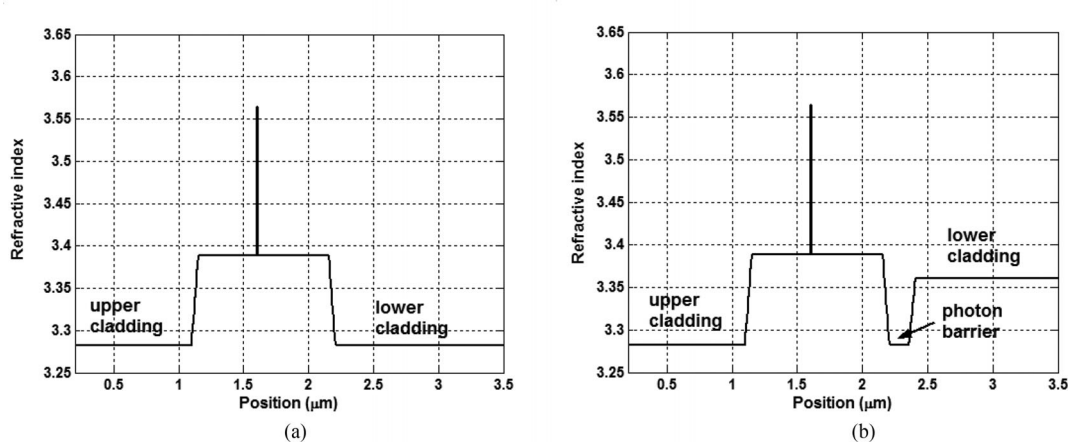

Fig. 1. Diagram of designed waveguide structure A (a) and structure B (b). Structure A is a conventional LOC waveguide, and structure B is with an incorporation of a tunneling waveguide.

as thick as a few microns. The very thick waveguide makes it likely to support more than one modes, and this would lead to the possibility of lasing from the higher-order modes. If this occurs, the L-I characteristics as well as beam quality will become deteriorated. To maintain single mode operation in the vertical direction in LOC waveguide configurations, efforts have been made, for example by using very small difference in the refractive indices between the waveguide and the cladding materials [7]. The difference can be as small as 0.04, and this would leads to much lower quantum confinement factor for the fundamental mode and hence higher threshould current. In addition, the growth tolerance could also be affected.

In this paper, we present detailed study of the effect of LOC waveguide design on the laser's kink performance and it was found that a multi-mode waveguide in the epi growth direction could lead to the occurrence of the power kink in the L-I curves, and the occurrence of the power kink was accompanied with broadening of the beam divergence in the wafer growth direction. In order to eliminate the kink issue [8] that was associated with the higher order mode lasing, a higher order mode tunneling waveguide structure was implemented. The tunneling waveguide works for photons in analogy to that a quantum well works for electrons, in which only fundamental wave function can exist, and higher order wave functions will no longer exist because of the strong tunneling effect. Test of our fabricated devices in which the tunneling waveguide was incorporated, shows very stable beam divergence against the variation in the injection current and excellent L-I linearity, indicating the lasers with the new design indeed operated in the single mode regime.

2. Single Mode LOC Waveguide Design

In this section, we will describe the laser epitaxy design concepts. To facilitate our experimental study, we have designed two types of epi structures based on AlGaAs material system, referred to as structure A and structure B (see Fig. 1), respectively. Fig. 2 shows simulated mode profiles, and Table 1 lists the correspondent effective indices for structure A. From the calculation, we can see that structure A supports three waveguide modes. We will show later that in a multimode waveguide structure, lasing operation could become unstable because of higher order mode lasing. In order to remove higher order modes, and in the meantime to minimize impact on the fundamental mode profile, we modified the structure A by replacing part of lower cladding material in the structure A with the material that has higher index, [see Fig. 1(b)]. The purpose of using higher index material is to enable strong mode leakage (analogy to the electron tunneling in quantum wells) to take place. Clearly to make the higher order mode tunneling happen, the refractive index of the material that is further away from the active region needs to be larger than the effective index of the 1st mode shown in Table 1. In our design, we choose the refractive index of the tunneling layer to be

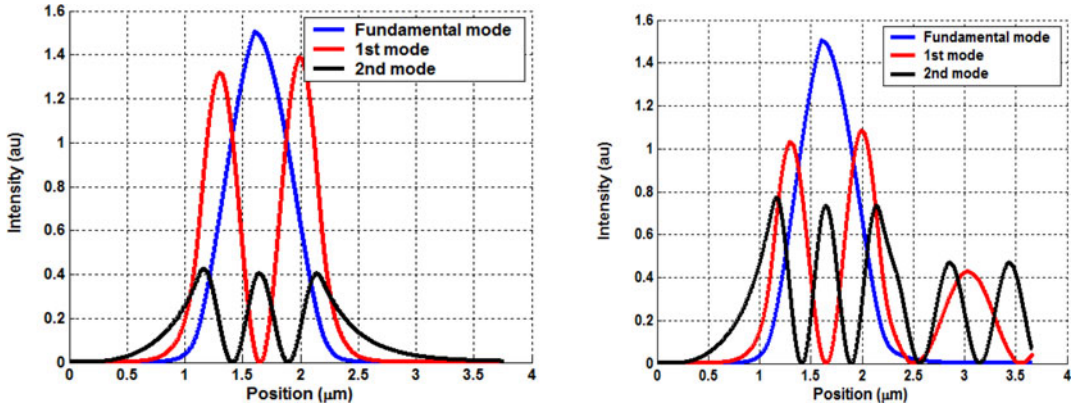

Fig. 2. Simulated mode profiles for structure A (left) and Structure B (right).

TABLE 1
The Effective Refractive Indices for the Waveguide Modes of Structure A

Waveguide mode	Effective refractive index
Fundamental mode	3.37765
1st mode	3.33858
2nd mode	3.28834

3.36 which is equivalent to that of Al0.41GaAs. Waveguide simulation shows structure B is indeed single-moded, because of the strong tunneling effect for the higher order modes. In order for one to clearly view the tunneling effect, we plot the mode profile of the fundamental mode for structure B along with the two modes that have the effective indices respectively equal to those for the 1st and 2nd mode for structure A. From the plot, one can see higher order modes in the structure B are no longer fully confined because of strong leakage. Obviously, the thickness of the lower cladding layer which is next to the waveguide and will be referred to as the photon barrier thereafter for simplicity [see Fig. 1(b) for details] has to be chosen very carefully, because if the layer is too thin, the fundamental mode profile will be impacted and if it is too thick, the tunneling effect will be weakened. To quantitatively characterize the effect of the photon barrier layer thickness, we calculated the mode overlap factor C between the fundamental modes for the structure A and structure B. The overlap factor is defined as:

$$C = \frac{\int I_1(y) I_2(y) dy}{\left(\int I_1(y) I_1(y) dy \int I_2(y) I_2(y) dy\right)^{1/2}} \quad (1)$$

where I_1 and I_2 are the fundamental mode distributions for the structure A and structure B respectively. Obviously, if the two modes have exactly identical profiles, the overlap factor will be equal to 1, and if there is no overlap at all, the factor will be equal to zero. Fig. 3 plots the calculated quantum well confinement factor of the fundamental mode for structure B, and the mode overlap factor between the fundamental modes in structure A and structure B (black curve) as a function of the photon barrier layer thickness. From the calculation, one can see the mode-overlap factor approaches to 1 when the photon barrier layer thickness is more than 100 nm. In the meanwhile, the quantum confinement factor is also very close to its maximum, indicating the tunneling layer has very little impact on the fundamental mode. Fig. 4 plots the fundamental mode profiles for

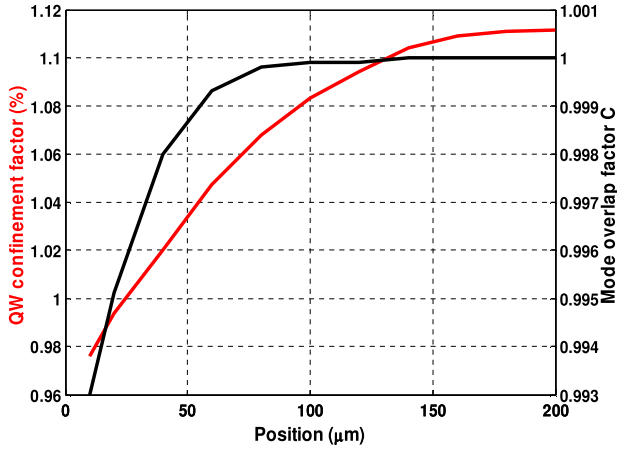

Fig. 3. Calculated quantum well confinement factor of the fundamental mode in structure B (red curve), and mode overlap factor C for the fundamental modes in structure A and structure B (black curve) as a function of the photon barrier layer thickness.

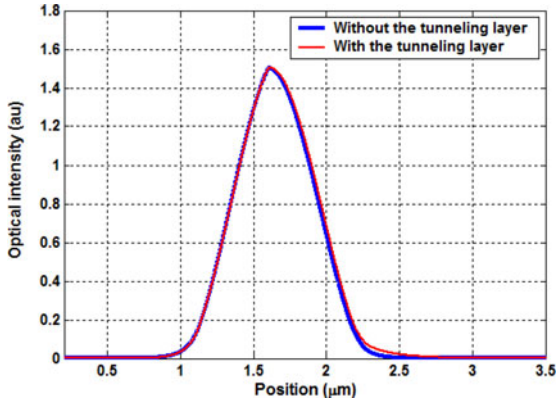

Fig. 4. Calculated fundamental mode profiles for structure A (blue) and structure B (red).

the two types of structures where the photon barrier layer thickness was chosen to be 150 nm in structure B, from which one can see the two fundamental modes have almost the same profiles. To further examine the tunneling effect, the tunneling probability was calculated using the following simplified formula:

$$T = \exp\left(-2\int_{\Delta d} K_0\sqrt{n_e^2 - n_b^2}\,dy\right) \tag{2}$$

where T denotes the photon tunneling probability, K_0 is the wave number in the free space, n_e is the effective index of a waveguide mode, n_b is the effective index of the photon barrier material, and Δd is the thickness of the photon barrier layer. Fig. 5 plots the dependence of tunneling probability on the photon barrier thickness for the higher order modes in structure B, from which one can see that when the layer thickness is 100 nm, the tunneling probability is over 30%. In our design, we chose the thickness of the photon barrier layer to be 150 nm in structure B.

3. Fabrication

The epitaxy materials for both the structure A and structure B were grown using MOCVD and both epitaxial structures contain an identical InGaAlAs single quantum well (SQW) sandwiched

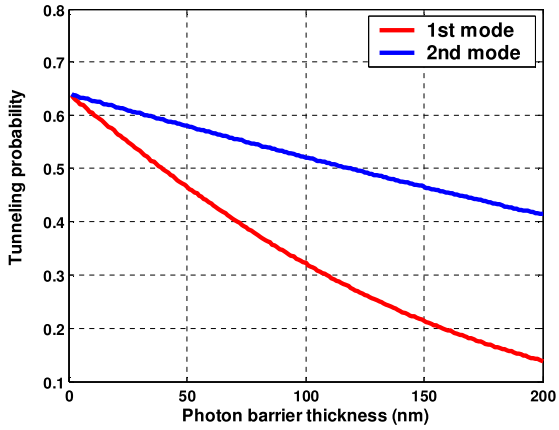

Fig. 5. Calculated tunneling probability for the first and second higher order modes.

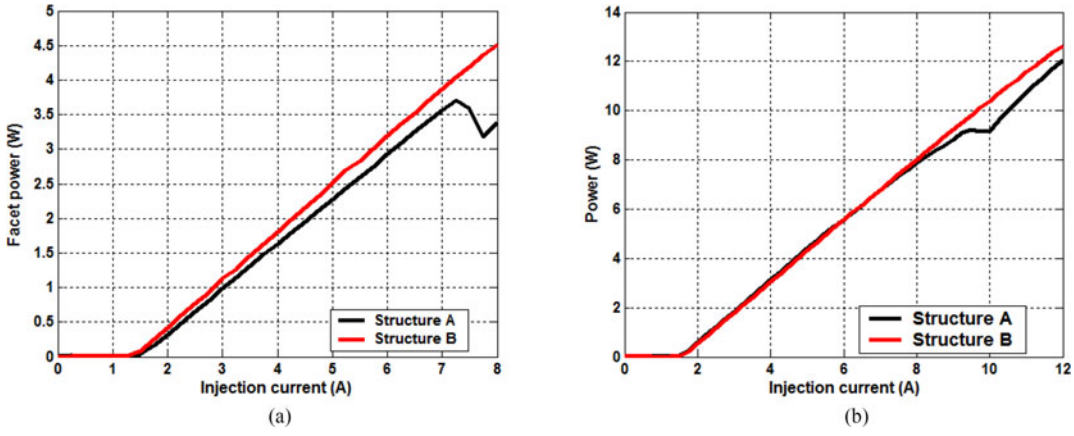

Fig. 6. Measured light-current dependence for uncoated devices (a) and the coated devices (b).

between two separate confinement heterostructure (SCH) AlGaAs layers. N-doping and p-doping were optimized such that the lasers could produce highest energy conversion efficiency which was around 62% by calculation, when the operation current is 12 A. The length of chips is 2.5 mm long, and the aperture is 350 μm wide. The fabrication was performed using routine semiconductor processes including forming of the waveguide by wet-etching, p-metal contact, wafer thinning and n-metal contact etc. Facet coatings for high reflection (HR) and anti-reflection (AR) were finally performed with the HR reflectivity being about 99%, and AR reflectivity being around 7%.

4. Test

Device test was made using our COS-tester, which can perform, either at CW or at pulsed mode, the measurements of light-current-voltage (L-I-V), far-fields and optical spectrum at a controlled heat-sink temperature. In our test, measurements of laser parameters including L-I-V characteristics, far fields and the spectra were made in CW condition and the heat-sink temperature was set to 20 °C. The power was measured using an integrating sphere. Fig. 6 Shows measured L-I plots for uncoated and coated devices fabricated using structure A and structure B materials. Apparently, Devices from structure A show very notable power kink at the currents of around 8 A and 10 A for uncoated and coated devices respectively. In contrast, devices from structure B displays very good L-I linearity. From our test, it seemed that the position at which the kink appears is a bit random, but it always appeared somewhere when the injection current was above 7 A. Fig. 7 plots

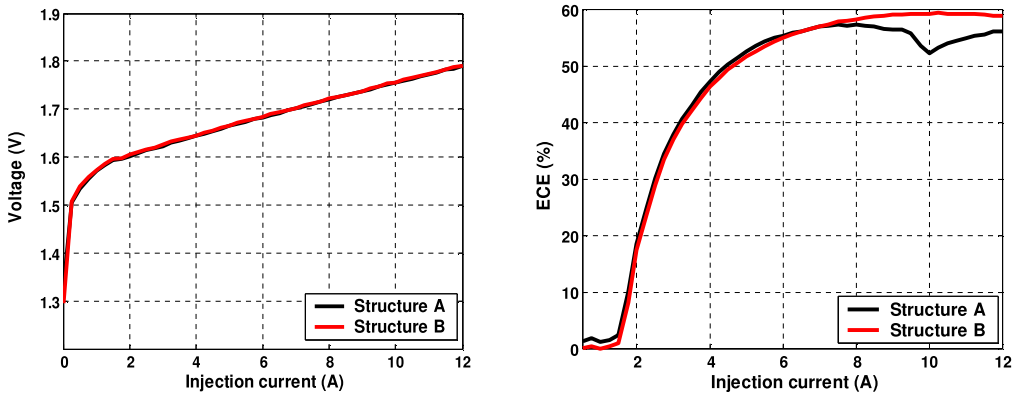

(a) (b)

Fig. 7. Measured I-V curves (a) and the energy conversion efficiency (b) for the both types of materials.

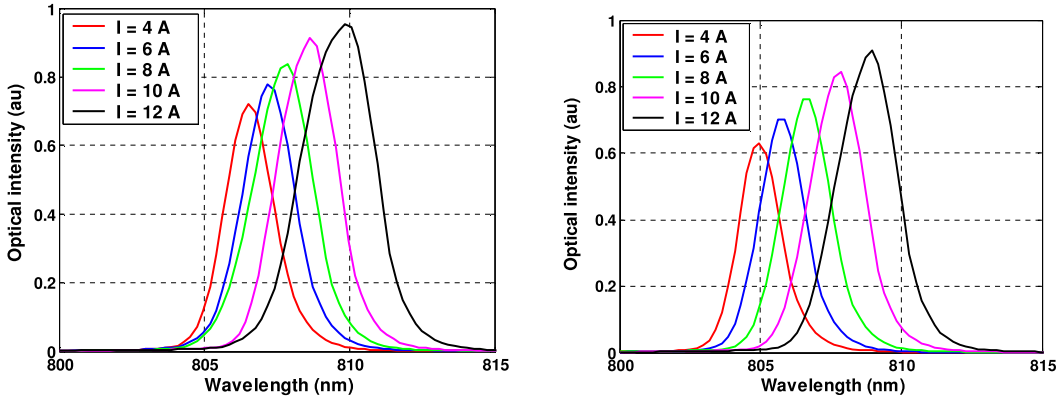

(a) (b)

Fig. 8. Measured spectra for the structure A (a) and the structure B (b).

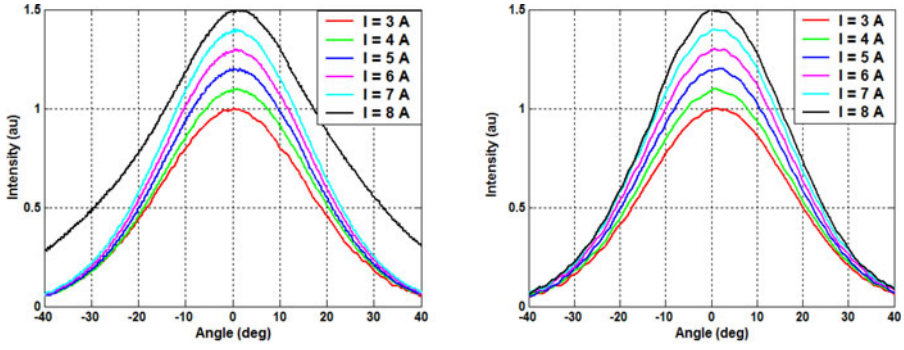

(a) (b)

Fig. 9. Measured far field profiles for structure A (a) and structure B (b) at different current levels.

the I-V characteristics as well as the energy conversion efficiency for the structures A and B, from which one can see the voltages for both structures are very close to each other, indicating that incorporation of the photon barrier layer does not affect the device's voltage characteristics and their efficiency. In order to further investigate the fundamental causes for the occurrence of the power kink, we also measured the far field profiles as well as wavelength spectra for both types of devices at different current injection levels, and it was found the spectra for both type of the devices

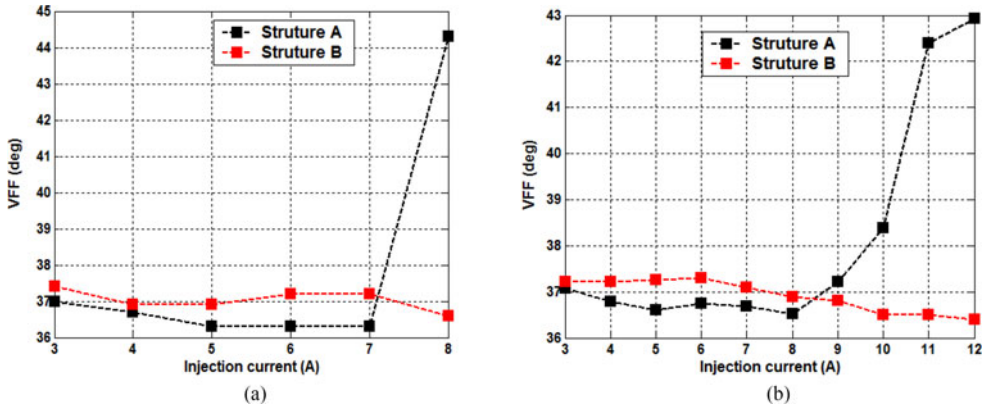

Fig. 10. Measured VFF FWHM values as a function of injection current for uncoated devices (a) and coated devices (b).

remained normal and similar to each other in the same current range (see Fig. 8). However, the far field profiles (see Fig. 9) along the wafer growth direction, which is referred as VFF, exhibit quite different behaviors. Indeed the beam divergence, which is defined as the full-width at the half maximum (FWHM), of devices using structure B remains around 37° for both coated and uncoated devices, which is compared to a large increase in the beam divergence at the kink points for devices with structure A (see Fig. 10). The occurrence of power kink which is accompanied with the far field broadening suggests that the higher order mode lasing takes place in lasers with structure A.

5. Summary

We demonstrated experimentally that a multimode LOC waveguide could cause higher order mode lasing, which in turn results in the occurrence of the power kink. In our improved design, we incorporated a photon tunneling mechanism to enable the waveguide only support fundamental mode, and in such a way, the power kink associated with the higher order mode lasing has been removed. Although we demonstrated our design concept in 808 nm lasers based on AlGaAs material system, the concept can be applied to other wavelengths and material systems as well.

References

[1] H. F. Lockwood, H. Kressel, H. S. Sommers Jr., and F. Z. Hawrylo, "An efficient large optical cavity injection laser," *Appl. Phys. Lett.*, vol. 17, no. 11, pp. 499–502, 1970.
[2] A. Knauer, G. Erbert, R. Staske, B. Sumpf, H. Wenzel, and M. Weyers, "High-power 808 nm lasers with a super-large optical cavity," *Semicond. Sci. Technol.*, vol. 20, no. 6, pp. 621–624, 2005.
[3] T. Morita *et al.*, "High-efficient and reliable broad-area laser diodes with a window structure," *IEEE J. Select. Topics Quantum Electron.*, vol. 19, no. 4, Jul./Aug. 2013, Art. no. 1502104.
[4] P. Crump *et al.*, "20W continuous wave reliable operation of 980 nm broad-area single emitter diode lasers with an aperture of 96 μm," *Proc. SPIE*, vol. 7198, 2009, Art. no. 719814.
[5] C. Schultz *et al.*, "11W broad area 976 nm DFB lasers with 58% power conversion efficiency," *Electron. Lett.*, vol. 46, pp. 580–581, 2010.
[6] P. Crump *et al.*, "975-nm high-power broad area diode lasers optimized for narrow spectral linewidth applications," *Proc. SPIE*, vol. 7583, 2010, Art. no. 75830N.
[7] P. Crump *et al.*, "Efficient high-power laser diodes," *IEEE J. Select. Topics Quantum Electron.*, vol. 19, no. 4, Jul./Aug. 2013, Art. no. 1501211.
[8] M. F. C. Schemmann *et al.*, "Kink power in weakly index guided semiconductor lasers," *Appl. Phys. Lett.*, vol. 66, pp. 920–922, 1995.